



HAL
open science

Satellite lines induced by electrons of near-threshold energy in the x-ray emission band spectra of 3d, 4d, and 5d transition metals

Philippe Jonnard, I. Jarrige, Christiane Bonnelle

► **To cite this version:**

Philippe Jonnard, I. Jarrige, Christiane Bonnelle. Satellite lines induced by electrons of near-threshold energy in the x-ray emission band spectra of 3d, 4d, and 5d transition metals. 2004. hal-00002265

HAL Id: hal-00002265

<https://hal.science/hal-00002265v1>

Preprint submitted on 22 Jul 2004

HAL is a multi-disciplinary open access archive for the deposit and dissemination of scientific research documents, whether they are published or not. The documents may come from teaching and research institutions in France or abroad, or from public or private research centers.

L'archive ouverte pluridisciplinaire **HAL**, est destinée au dépôt et à la diffusion de documents scientifiques de niveau recherche, publiés ou non, émanant des établissements d'enseignement et de recherche français ou étrangers, des laboratoires publics ou privés.

Satellite lines induced by electrons of near-threshold energy in the x-ray emission band spectra of $3d$, $4d$, and $5d$ transition metals

P. Jonnard,* I. Jarrige, and C. Bonnelle

*Laboratoire de Chimie Physique - Matière et Rayonnement,
Université Pierre et Marie Curie, UMR-CNRS 7614,
11 rue Pierre et Marie Curie, F-75231 Paris Cedex 05, France*

(Dated: July 22, 2004)

The $L\beta_2$ emission band ($4d \rightarrow 2p_{3/2}$ transition) of selected transition metals of the $4d$ series (Y, Zr, Mo, and Ru) is studied under electron impact. Several spectra are recorded with electron energies as low as 15 eV above the $2p_{3/2}$ threshold. A satellite line is observed towards the high photon energy side of the normal emission. As the incident electron energy decreases and approaches the threshold energy of the emission, the intensity of the satellite line relatively to that of the normal emission line increases. The satellite has also been observed above the emission bands of $3d$ (Fe) and $5d$ (W) elements. In contrast, in the case of Ag, the above satellite line has not been observed. Thus, its existence is common to all the nd elements having an open d shell. The satellite is interpreted as due to a transition in an ionized atom having an additional d hole in its valence band ($nd^{-2} \rightarrow n'p_{3/2}nd^{-1}$ transition).

PACS numbers: 78.70.En, 34.80.Dp, 71.20.Be

I. INTRODUCTION

The high energy satellites of the x-ray emission bands in metals have received little attention. These satellites are due to transitions in doubly- or multiply-ionized atoms. A two-electron excitation or ionization is generally described as a shake process. In this process, the ejection of the second electron is due to the rearrangement of the atomic electrons during the creation of the core hole. The intensity of shake-up satellites vanishes at the double excitation threshold and increases rapidly beyond it up to an intensity saturation, at about twenty percents of the parent emission intensity.¹

For molybdenum, we have observed a particular behaviour of the high energy satellite of the $L\beta_2$ ($4d \rightarrow 2p_{3/2}$ transition) emission band²: close to the $2p_{3/2}$ ionization threshold, the satellite is more intense than the parent line. Its relative intensity with respect to the emission band reaches a maximum near the threshold and decreases beyond. In contrast, for an excitation energy E of the order of twice the threshold, the intensity of the satellite is negligible with respect to that of the parent line.

We show that this resonant-like behaviour of the emission band satellite is characteristic of the transition elements. These elements have particular properties due to the presence of an open d subshell. A high density of empty nd states is present inside a narrow energy interval about ten eV large, just above the Fermi limit. The $d-d$ low-energy excitations induce intense transitions in the optical spectra. In x-ray emission spectroscopy, one expects these excitations to have an important role, when the core-hole is produced with incident particles having an energy close to the threshold energy.

Studies close to the ionization threshold have been performed with monochromatic photon excitation, essentially for compounds.^{3,4} Satellites of the emission bands

have been observed but they have received little attention because the spectra are complex close to the threshold, and discussion concerns essentially the inelastic scattering features, *i.e.* the shift of the emission band with the variation of the incident energy. When the incident particles are electrons of energy E just above the energy of double excitation, the parent and satellite emissions are observed simultaneously. Thus, their relative intensity can be measured.

We present here an experimental study of the high energy satellite of the $2p_{3/2} - nd$ emission band for transition metals with $n = 3$ (Fe), $n = 4$ (Y, Zr, Mo² and Ru), and $n = 5$ (W), and also for Ag. The excitation is performed by low energy electrons. Importance is given to the $4d$ elements because the $2p$ spin-orbit coupling is large. The study concerns metals because they are simple systems with no charge transfer, and the densities of their d states is well known. The relative intensity of the satellite with respect to the parent emission is determined as a function of the excitation energy, E , in a large energy range from 15 eV above the double threshold up to about three times the threshold.

II. EXPERIMENTAL

The Mo sample is either a 99.9% purity plate, or a 1 μm thick film deposited by magnetron sputtering on a silicon substrate. The compounds MoO₃ (powder from Rhône Poulenc), and Mo₅Si₃ (powder of 99.5% purity from Alfa Aesar) are also analyzed. The Y sample is a 99.9% purity plate from A.D. Mackay Inc. The Zr and Fe samples are 99.9% purity plates. The Ru sample is a metallic powder, of unknown purity, from Touzart & Matignon. The Ag sample is a thick film, deposited by thermal evaporation from a 99.999% purity foil from Johnson Matthey. The W sample is a 1 μm thick film deposited by magnetron

sputtering on a silicon substrate. The sputtered films are prepared from 99.9% or better purity targets. The plates are polished to obtain an optical finish. All the samples are glued on a water-cooled sample holder which is chosen not to produce an x-ray emission in the spectral range of interest.

The studied emission bands which take place from the nd valence states are (see also Table I) :

- the $L\beta_2$ emission ($4d \rightarrow 2p_{3/2}$ transition) for the $4d$ elements;
- the $L\alpha$ emission ($3d \rightarrow 2p_{3/2}$ transition) for the $3d$ elements (Fe);
- the M_3O_5 emission ($5d \rightarrow 3p_{3/2}$ transition) for the $5d$ elements (W).

For Zr and Mo, the $L\alpha$ emission ($3d \rightarrow 2p_{3/2}$ transition) is also studied to compare the behavior of the satellite of this line with that of the $L\beta_2$ satellite line. The $L\alpha$ emission involved the same core level as the $L\beta_2$ emission, but takes place from the $3d$ core level and not from the valence band (see Table I). For Fe, the $L\beta$ emission ($3d \rightarrow 2p_{1/2}$ transition) is also recorded. In the Table I are indicated the experimental values of the maximum of the various studied emissions, taken from Ref. 5, and of the binding energy levels, taken from Ref. 6.

It is important to know for which electron energy the emission becomes observable, *i.e.* which is the energy threshold of the emission. This energy cannot be directly determine by reading the high voltage applied to accelerate the electrons, because one needs to know :

- the work function of the cathode used to produce the electrons;
- the thermal distribution of the electrons due to the heating of the cathode;
- the offset between the read and actual applied voltage.

We have determined experimentally this energy in the case of Mo, by using the Mo $L\alpha$ emission which is the most intense emission of the Mo L-spectrum, and has the same ionization limit as the $L\beta_2$ emission. This emission is recorded with decreasing electron energies until no emission can be observed. Close to the threshold the energy step is 5 eV. This enables to determine the difference between the applied high voltage and the Mo $2p_{3/2}$ threshold energy within a ± 2.5 eV uncertainty. This difference is added to all the electron energies. We present in Fig. 1 some Mo $L\alpha$ spectra obtained above and below the ionization limit.

The electron energies used to obtained the emissions involving the nd valence states are presented in Table II for the $4d$ transition metals, for Ag, and for the $3d$ (Fe), and $5d$ (W) elements. The electron energies are chosen to perform the spectrum acquisition with overvoltages, *i.e.* the ratio of the electron energy to the threshold energy,

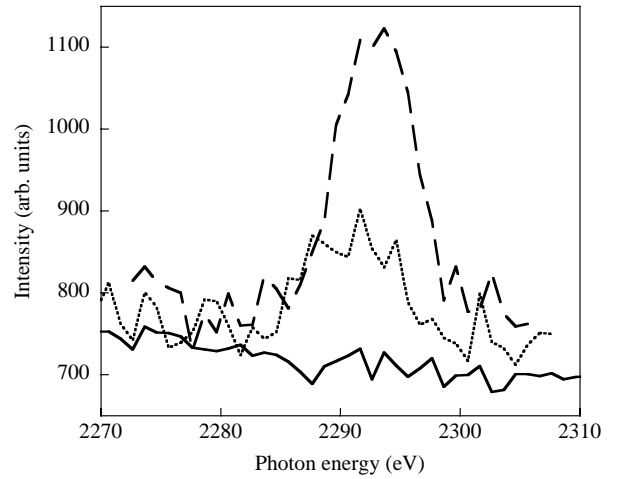


FIG. 1: Mo $L\alpha$ emission for various electron energies close to and below the Mo $2p_{3/2}$ threshold (2520 eV). Solid line : 2515 eV; dotted line : 2525 eV; dashed line : 2535 eV.

between ≈ 2.4 and ≈ 1.1 . In the case of Mo, some spectra are acquired with overvoltages as low as 1.006.

The analyzed thickness, *i.e.* the thickness which contributes 80% of the x-ray intensity, is calculated by a semi-empirical model devoted to the modelisation of the generation of characteristic x-rays in solids irradiated by electrons.⁷ This model takes into account the energy and angular distributions of the transmitted and backscattered electrons, the ionization cross sections by electrons, and the absorption of the photons inside the sample. It is specially designed to work at low electron energies (down to 500 eV), and overvoltages as low as 1.02. The calculated values are reported in Table II.

It is well known that the reabsorption of the photons emitted in metallic samples can distort the shape of the emission bands. This is due to the strong variation of the absorption coefficient around the absorption edge, located at the top of the valence band. In our study, the electrons have a low energy, and they penetrate only a small thickness (see Table II). Then, the reabsorption effect is negligible. For example, in the case of Mo, we have calculated that, for electrons with energy of 6000 eV, the reabsorption effect can modify the relative intensity of the features below and above the top of the valence band by 16%, at 3000 eV by 2%, and has no significant effect below this energy. We have also verified, at 3000 eV electron excitation, that the shape of the emission is almost independent of the angle between the detection direction of the x-rays and the sample surface, *i.e.* independent of the distance travelled by the x-rays inside the sample.

The spectra are acquired with the IRIS apparatus,⁸ where the sample is under high vacuum (10^{-6} Pa or less) during the acquisition. The sample is irradiated by an electron beam produced by a Pierce gun. Because of the low pressure and the low electron current density (≈ 1 mA/cm²), the samples are unaffected by the electron irradiation. This is verified by checking that the

TABLE I: Data concerning the studied elements, and the studied emission bands and lines.

Z	element	emission	transition	energy (eV) ^a	binding energies (eV) ^b					
4d					$2s$	$2p_{1/2}$	$2p_{3/2}$	$4s$	$4p_{1/2}$	$4p_{3/2}$
39	Y	$L\beta_2$	$4d \rightarrow 2p_{3/2}$	2077.8 ^c	2373	2156	2080	43.8	24.4	23.1
40	Zr	$L\beta_2$	$4d \rightarrow 2p_{3/2}$	2219.4	2532	2307	2223	50.6	28.5	27.1
		$L\alpha$	$3d \rightarrow 2p_{3/2}$	2043.0						
42	Mo	$L\beta_2$	$4d \rightarrow 2p_{3/2}$	2518.3	2866	2625	2520	63.2	37.6	35.5
		$L\alpha$	$3d \rightarrow 2p_{3/2}$	2293.2						
44	Ru	$L\beta_2$	$4d \rightarrow 2p_{3/2}$	2836.0	3224	2967	2838	75.0	46.3	43.2
47	Ag	$L\beta_2$	$4d \rightarrow 2p_{3/2}$	3347.8	3806	3524	3351	97.0	63.7	58.3
3d					$2s$	$2p_{1/2}$	$2p_{3/2}$	$3s$	$3p_{1/2}$	$3p_{3/2}$
26	Fe	$L\alpha$	$3d \rightarrow 2p_{3/2}$	704.95	844.6	719.9	706.8	91.3	52.7	52.7
		$L\beta$	$3d \rightarrow 2p_{1/2}$	717.95						
5d					$3s$	$3p_{1/2}$	$3p_{3/2}$	$5s$	$5p_{1/2}$	$5p_{3/2}$
74	W	M_3O_5	$5d \rightarrow 3p_{3/2}$	2275.2	2820	2575	2281	75.6	45.3	36.8

^afrom Ref. 5.^bfrom Ref. 6.^cnot in the tables of x-ray wavelengths : determined experimentally.

emission shape and intensity are stable during the acquisition.

The x-ray analysis is performed with a high resolution x-ray spectrometer working with bent crystals of 500 mm radius. The analyzing crystal is InSb (111), used in the first diffraction order for all the emissions, except for the Fe L emissions, obtained with a TiAP (001) crystal in the first diffraction order, and the Ag $L\beta_2$ emission, obtained with a quartz (10 $\bar{1}0$) crystal in the second diffraction order.

The x-ray detector is of Geiger-type, working with a Ar-CH₄ gas flux. Because many experiments are performed close to the threshold, *i.e.* with a small number of emitting atoms and low ionization cross sections, the slit in front of the detector is wide open in order to increase the intensity at the expense of the resolution. However, the relative resolution $\Delta h\nu/h\nu$ is between 500-1000, depending on the studied emissions, which still allows, in most of the cases, to easily resolve the satellite emission from its parent line.

III. RESULTS

A. 4d transition metals

1. Mo

The presented spectra are obtained by subtracting a linear background from the original spectra. In the case of the two lowest electron energies (2535 and 2545 eV), this was not possible because of the presence of the short wavelength limit (SWL), which manifests itself as a discontinuity towards the high photon energy side of the

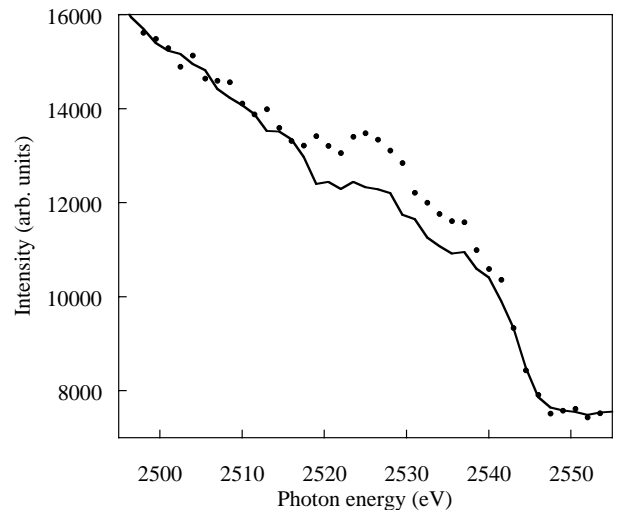


FIG. 2: Mo $L\beta_2$ emission obtained with 2535 eV electrons (dots), and shifted background obtained with 2500 eV electrons (line).

spectrum. The background corresponding to these spectra was acquired with 2500 eV electrons impinging on the Mo sample. In this case, the electrons do not have sufficient energy to induce the $L\beta_2$ emission, but the SWL is present. Then, the spectrum obtained at 2500 eV is shifted in energy to match the SWL of the spectra obtained at 2535 and 2545 eV, and then subtracted from these latter. This is shown in Fig. 2 for the lowest incident electron energy. This procedure enables to suppress the structures in the background, which, close to the SWL, are related to the unoccupied density of states.

The Mo $L\beta_2$ emission spectrum obtained with various

TABLE II: Relative intensities of the studied emissions of the 4d transition metals. E is the electron energy. $x_{80\%}$ is the thickness that contributes 80% of the x-ray intensity. The overvoltages E/E_0 , and the excess energies, $E - E_0$, above the binding energy of the core level involved in the emission, E_0 (Table I), are also indicated.

Z	element	E (eV)	$x_{80\%}$ (nm)	E/E_0	$E - E_0$	
4d						
						$I(L\beta_2)/I(\text{sat})$
39	Y	4815	82.0	2.31	2735	6.5
		2365	9.9	1.14	285	-
40	Zr	5015	60.6	2.26	2792	-
		2515	7.4	1.13	292	0.76
		2285	3.2	1.03	62	-
42	Mo	6015	53.0	2.39	3495	-
		3015	8.3	1.20	495	10.2
		2665	3.8	1.06	145	1.3
		2630	3.2	1.04	495	0.51
		2575	2.7	1.022	55	0.35
		2565 ^a	-	1.018	45	-
		2555 ^a	-	1.014	35	-
		2545 ^a	-	1.009	25	-
2535 ^a	-	1.006	15	-		
44	Ru	6515	49.5	2.30	3677	-
		3215	5.9	1.13	377	6.9
		2945	2.7	1.03	107	2.3
47	Ag	7515	73.5	2.24	4164	-
		3795	9.2	1.13	444	-
		3505	4.0	1.05	154	-
3d						
						$I(L\alpha)/I(\text{sat})$
26	Fe	2508	19.0	3.56	1801	-
		1208	5.3	1.72	501	2.8
		828	1.8	1.17	121	1.9
		758	1.1	1.07	51	1.3
		743	1.0	1.05	36	1.1
5d						
						$I(M_5O_5)/I(\text{sat})$
74	W	5515	27.3	2.42	3234	2.9
		2805	5.0	1.23	524	0.75

^atoo small overvoltage to perform the calculation of the emissive thickness.

incident electrons energies, ranging from 6015 to 2535 eV, *i.e.* only 15 eV above the Mo $2p_{3/2}$ threshold are shown in Fig. 3. The first series obtained with the most energetic electrons, Fig. 3a, is acquired with a 250 μm wide slit placed in front of the detector. The second series obtained with the less energetic electrons, Fig. 3b, is acquired with a 1000 μm wide slit, in order to increase the collected intensity. This explains the poorer spectral resolution of this series.

In Fig. 3a the $L\beta_2$ emission, obtained with electron energies between 6015 and 2630 eV, are normalized with respect to the maximum of the $L\beta_2$ emission. At 6015 eV, a rather symmetric band is observed. It is related to the occupied 4d density of states (DOS). As the electron energy decreases, a satellite structure appears about 8 eV above the main line, and increases in intensity. This structure is located well above the top of the valence band (2520 eV), and cannot be related to a feature of the DOS of Mo. At

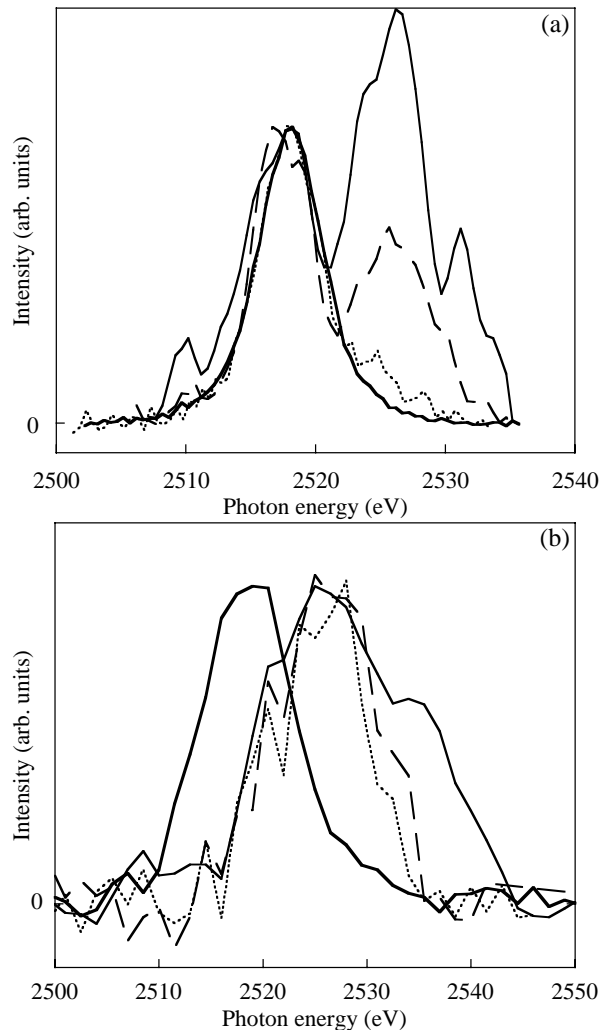


FIG. 3: Mo $L\beta_2$ emission of Mo metal for various electron energies. (a) Thick solid line : 6015 eV; dotted line : 3015 eV; dashed line : 2665 eV; thin solid line : 2630 eV. (b) Thick solid line : 3015 eV; dotted line : 2565 eV; dashed line : 2555 eV; thin solid line : 2535 eV.

2630 eV energy of the incident electrons, the intensity of the satellite is larger than that of the main line.

We present in Fig. 3b the $L\beta_2$ emission obtained with electron energies lower than 2565 eV. The spectrum obtained at 3015 eV is presented for comparison. The spectra are normalized with respect to their maximum. At the lowest electron energies, the normal line is not strong enough to rise up from the background. With the electron energy decreasing, the satellite line is observed to broaden towards the high photon energies. The large variation in broadening observed between the spectra obtained at 2555 and 2535 eV electron energies can be due in part to an imperfect background removal. This may lead to an overestimate of the satellite intensity.

In order to confirm that the observed structure around 2525-2535 eV is not due to the emission from the molybdenum atoms, which could be present in an oxide envi-

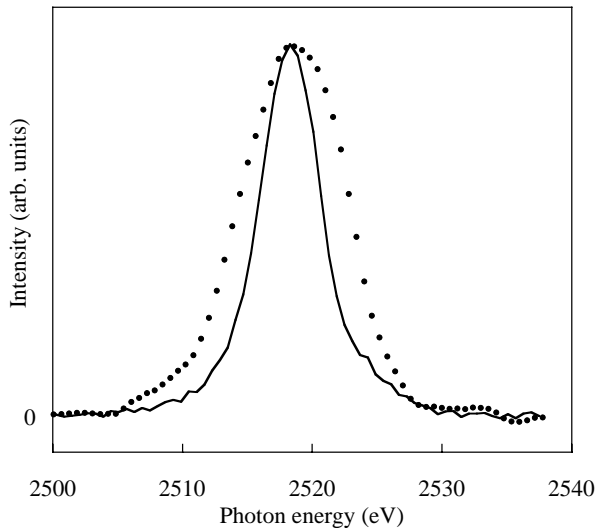


FIG. 4: Mo $L\beta_2$ emission obtained with 6015 eV electrons on Mo metal (line), and the oxide MoO_3 (dots).

ronment in the superficial analyzed zone, we present in Fig. 4 the comparison of the $\text{Mo}L\beta_2$ emissions of metal Mo and MoO_3 . They are obtained with a 6015 eV electron energy. Both spectra present the same maximum energy, but the spectrum of the oxide is broader than that of the metal. No structure is present in the photon energy range 2525-2535 eV in the spectrum of the oxide. This is also the case for solid solutions of Y_2VMoO_7 , and $\text{SrV}_{1-x}\text{Mo}_x\text{O}_3$,⁹ and for compounds where the Mo atoms are bound with ligands other than O atoms.^{10,11} These comparisons rule out the attribution of the satellite to a superficial molybdenum oxide or compound.

The intensity of the $L\beta_2$ emission increases with the incident electron energy, E , following a law of $(E - E_0)^{1.6}$, where E_0 is the threshold energy, *i.e.* the Mo $2p_{3/2}$ binding energy in this case. This is the classical behavior for the normal emissions of transition metals.¹² The intensity variation of the satellite line as a function of the electron energy is shown in Fig. 5. The points are scattered because close to the threshold the collected intensity is low, leading to a large uncertainty in the satellite intensity. There is also a large uncertainty in the value at 3015 eV, because the satellite line is unresolved from the parent line. However, a power law behavior with the same exponent as that of the parent line is excluded.

The ratio of the satellite line intensity to that of the normal line is measured for the first series of electron energies, except 6015 eV where the satellite is not observable. The corresponding values are reported in the Table II. As expected from the different power law behaviors of these emissions, the relative intensity of the satellite increases with the decreasing electron energy.

The Mo $L\beta_2$ emission of Mo_5Si_3 obtained with 6015 and 2815 eV electrons is shown in Fig. 6. The spectra are normalized with respect to their maximum. In this case, when the electron energy decreases, no satel-

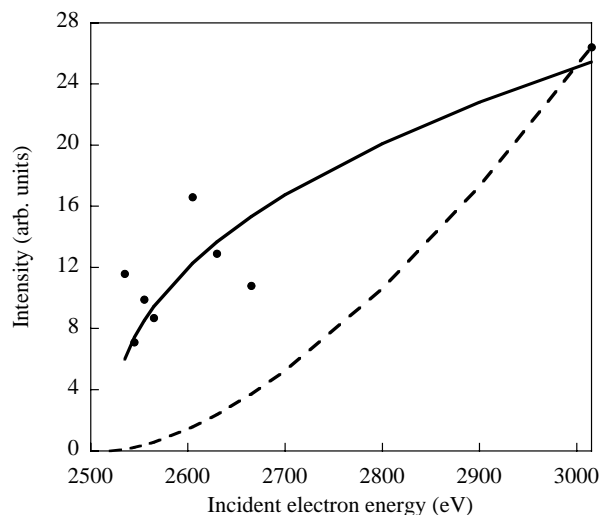


FIG. 5: Power law fit (solid line) of the intensity of the satellite line of the Mo $L\beta_2$ emission as a function of the electron energy (dots). The dashed line is a power law with the same exponent (1.6) as that of the normal line.

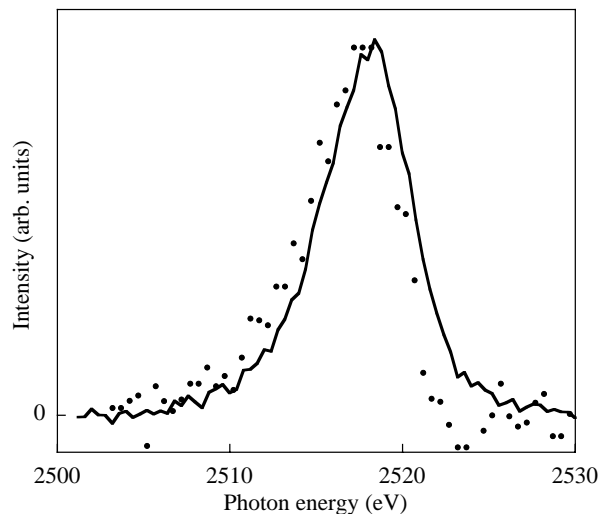


FIG. 6: Mo $L\beta_2$ emission of Mo_5Si_3 , obtained with 2815 (dots), and 6015 eV (line) electrons.

lite structure appears towards the high photon energies. If the satellite line should be present, the interpolation of the values in the Table II would lead to a relative intensity $I(L\beta_2)/I(\text{sat})$ of about 5, making the satellite easily observable. The slight evolution of the Mo $L\beta_2$ shape is probably due to a change in composition at the surface of the grains of the powder.

The Mo $L\alpha$ emission of Mo metal obtained with 6015 and 2715 eV electrons is shown in Fig. 7. This emission involves the same core level as the $L\beta_2$ emission but a different d level, lying in the core shells. A linear background is subtracted from the original spectra. The spectra are normalized with respect to their maximum. At high electron energy, a satellite located at high photon

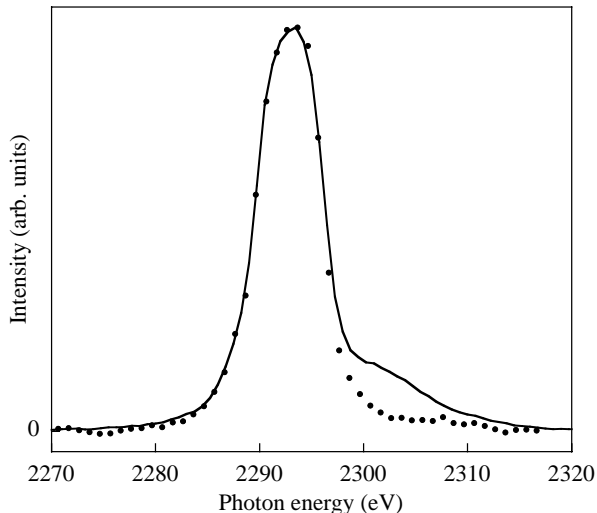


FIG. 7: Mo $L\alpha$ emission of Mo metal, obtained with 2715 (dots), and 6015 eV (line) electrons.

energy is clearly seen, about 10 eV above the parent line. With 2715 eV incident electrons, *i.e.* below the Mo $2s$ threshold, this satellite almost disappears, showing the opposite behaviour of the satellite of the $L\beta_2$ band.

2. Y, Zr, Ru, Ag

We present in Fig. 8a the $L\beta_2$ photon energy range obtained with the Y sample at a 4815 eV electron energy. The Y $L\beta_2$ emission is not reported in the tables of x-ray wavelengths. Indeed, there are two main lines in the photon energy range⁵ :

- the $L\beta_4$ emission ($3p_{1/2} \rightarrow 2s$ transition) located at 2060 eV;
- the $L\beta_3$ emission ($3p_{3/2} \rightarrow 2s$ transition) located at 2072 eV.

The $L\beta_2$ emission is only seen as a shoulder towards the high energy side of the $L\beta_3$ emission. Some satellite of the $L\beta_3$ emission could be expected in this photon energy range, but not with the intensity of the observed shoulder. The $L\beta_{3,4}$ doublet is fitted by two lorentzian curves, see Fig. 8a, whose widths are equal to the sum of the widths of the core level involved in the transitions and the experimental broadening. By subtracting this fit from the original spectrum, the "pure" $L\beta_2$ emission spectrum is obtained, Fig. 8b. Its energy at the maximum is 2077.8 eV, *i.e.* about 2 eV below the top of the valence band, whose energy is equal to the binding energy of the Y $2p_{3/2}$ level (Cf. Table I). This determination is in agreement with a previous observation,¹³ following a similar procedure. It can be seen that a satellite line is present around 2085 eV. Its intensity, relative to that of the parent line is indicated in Table II. The small in-

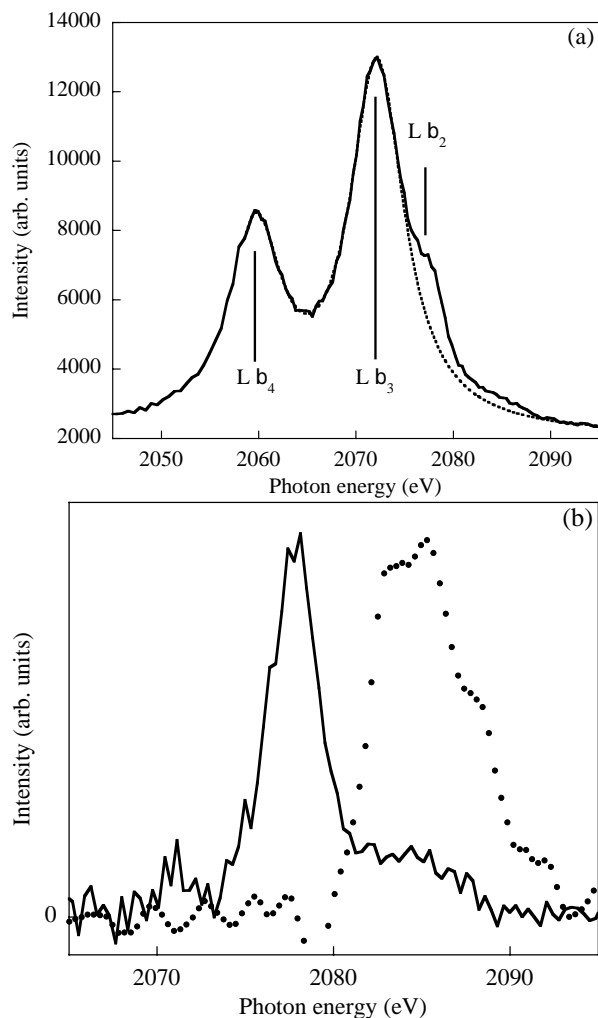


FIG. 8: Y $L\beta_2$ photon energy range of Y metal. (a) Original spectrum obtained with 4815 eV electrons (solid line), and fit of the $L\beta_{3,4}$ doublet (dotted line). (b) Treated spectrum obtained with 4815 eV electrons (line), and spectrum obtained with 2365 eV electrons (dots).

tensity structure seen at 2071 eV, is probably due to an imperfect subtraction of the $L\beta_{3,4}$ doublet.

The $L\beta_2$ photon energy range obtained with 2365 eV electrons is shown in Fig. 8b, and compared with the treated spectrum obtained at 4815 eV. The $L\beta_{3,4}$ doublet cannot be observed with 2365 eV electrons, because this energy is lower than the Y $2s$ binding energy (Table I). The $L\beta_2$ emission is not seen because its intensity is too low. This low intensity results from the small number of d electrons present in the yttrium atoms. A rough estimate of the $L\alpha$ to $L\beta_2$ ratio obtained at a 2.4 overvoltage leads to a value of 350 for Y, and of 30 for Mo. We present in Fig. 8b the spectrum after subtraction of a background fitted by a polynomial of the second order. There is a dip around 2079 eV, which is not explained. A structure is observed around 2085 eV, *i.e.* 7 eV above the $L\beta_2$ maximum. It is above the top of the valence band, at a

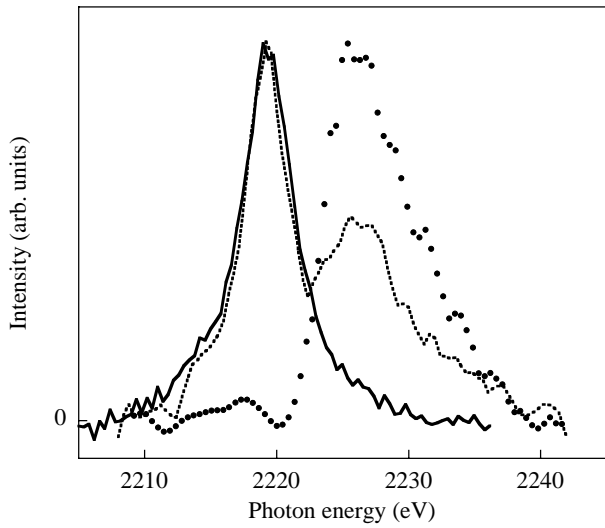


FIG. 9: Zr $L\beta_2$ emission of Zr metal, obtained with 2285 eV (dots), 2515 eV (dotted line), and 5015 eV (solid line) electrons.

distance comparable to that of satellite observed for Mo. Because the parent line is not detectable, the intensity ratio $I(\text{parent})/I(\text{satellite})$ cannot be determined.

The $L\beta_2$ emission of the Zr sample, obtained with 5015, 2515, and 2285 eV electrons is shown in Fig. 9. A linear background is subtracted from the original spectra. The curves are normalized with respect to their maximum. At the two lowest electrons energies, a satellite is present, at an energy of about 7 eV higher than the maximum of the parent line. At the lowest electrons energy, the normal line is not strong enough to rise up from the background. As before, this is due to the intrinsic low intensity of the $L\beta_2$ emission, due to the small number of d electrons in the zirconium atoms. A rough estimate of the $L\alpha$ to $L\beta_2$ ratio obtained at a 2.4 overvoltage leads to a value of 100. Similar to the Mo case, it is seen that as the incident energy of the electrons decreases, the intensity of the satellite decreases slower than that of the normal line. Because the satellite line is hardly detectable at 5015 eV, and the normal line vanishes at 2285 eV, the intensity ratio $I(\text{parent})/I(\text{satellite})$ can only be measured in the spectrum obtained with 2515 eV electrons. Its value is indicated in the Table II.

The Zr $L\alpha$ spectra, acquired with 5015 and 2285 eV electrons are shown in Fig. 10. They are normalized with respect to their maximum. The behavior of the $L\alpha$ emission is the same as that of Mo : the high energy satellite disappears when the electron energy decreases.

The $L\beta_2$ emission of the Ru sample, obtained with 6515, 3215, and 2945 eV electrons is shown in Fig. 11. A linear background is subtracted from the original spectra. The curves are normalized with respect to their maximum. The same phenomena observed for Mo, Y, and Zr takes place when the electron energy decreases : a satellite appears towards the high photon energy side of the normal line, and its relative intensity increases. In this

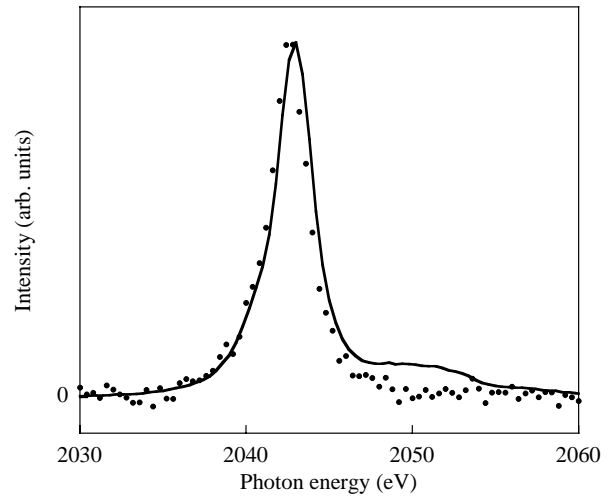


FIG. 10: Zr $L\alpha$ emission of Zr metal, obtained with 2285 eV (dots), and 5015 eV (line) electrons.

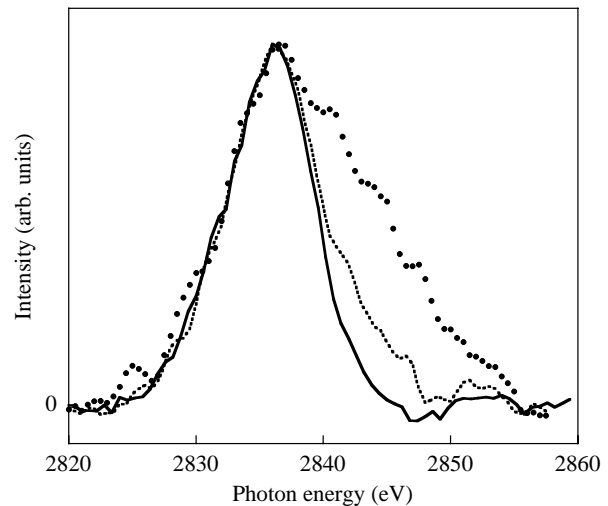


FIG. 11: Ru $L\beta_2$ emission of Ru metal, obtained with 2945 eV (dots), 3215 eV (dotted line), and 6515 eV (solid line) electrons.

case, the resolution is poor, and the satellite emission is not resolved from the parent line. However, by considering the spectrum obtained with the most energetic electrons as free of satellite, the position and intensity of the satellite has been determined on the spectra obtained with 2945 eV and 3215 eV electrons. Then, the satellite line lies 7.5 eV higher than the emission band maximum, and the intensity ratios $I(\text{parent})/I(\text{satellite})$ are indicated in the Table II.

The $L\beta_2$ emission of the Ag sample, obtained with 7515, 3795, and 3505 eV electrons is shown in Fig. 12. A linear background is subtracted from the original spectra. The curves are normalized with respect to their maximum. Contrary to what happens with the previously studied $4d$ elements, there is no appearance of a structure towards the high photon energy of the normal line

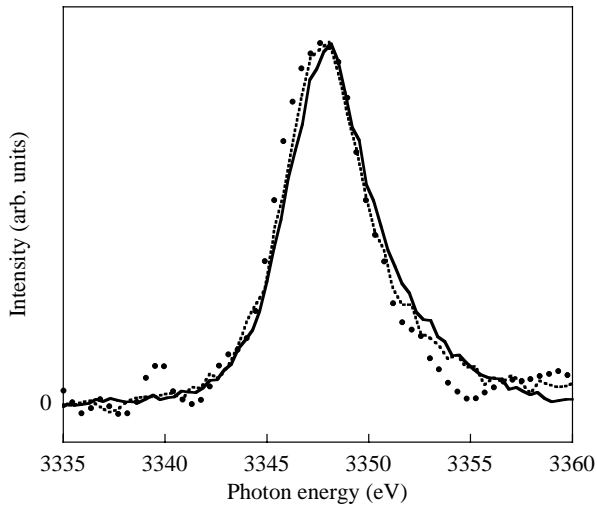


FIG. 12: Ag $L\beta_2$ emission of Ag metal, obtained with 3505 eV (dots), 3795 eV (dotted line), and 7515 eV (solid line) electrons.

when the incident electron energy is decreasing. It should be noted that, like the other studied $4d$ elements, the intensity of the Ag $L\alpha$ emission satellite decreases with the decreasing electron energy.¹⁴

B. $3d$ transition metals (Fe)

The $L\alpha$ and $L\beta$ emissions from the Fe sample is shown in the Fig. 13. The spectra obtained with various electron energies ranging between 2508 eV and 743 eV are normalized with respect to their maximum. In the spectrum obtained at 2508 eV, the $L\alpha$ emission is located at 705 eV, and the $L\beta$ emission at 718 eV. The spectrum is considered to be that of Fe metal, because of the large emissive thickness. By decreasing the electron energy, it is observed that the maximum of the $L\alpha$ emission shifts and broadens towards the high photon energies, as reported in Table III. The same kind of broadening, but less pronounced, is observed for the $L\beta$ emission.

From the small analyzed thickness with the less energetic electrons, one could expect the metal to be oxidized at its surface, and the evolution of the $L\alpha$ and $L\beta$ spectra to be due to a contribution of a superficial iron oxide. Indeed, when the oxidation degree of the iron atoms increases, a shift and a broadening of the $L\alpha$ emission are observed¹⁵ in the same way as those in our experiment as a function of the electron energy. This is studied by comparing the variations of the maximum and the width of the $L\alpha$ emission, and of the $L\alpha/L\beta$ intensity ratio (Table III), for the present experiment, and for Fe, FeO, and Fe₂O₃ from the literature.¹⁵ It can be seen that the magnitude of the shift and broadening of the $L\alpha$ emission as well as the $L\alpha$ to $L\beta$ intensity ratio are not compatible in the two experiments, see Table III. This definitively rules out the oxidation explanation. Only the variation

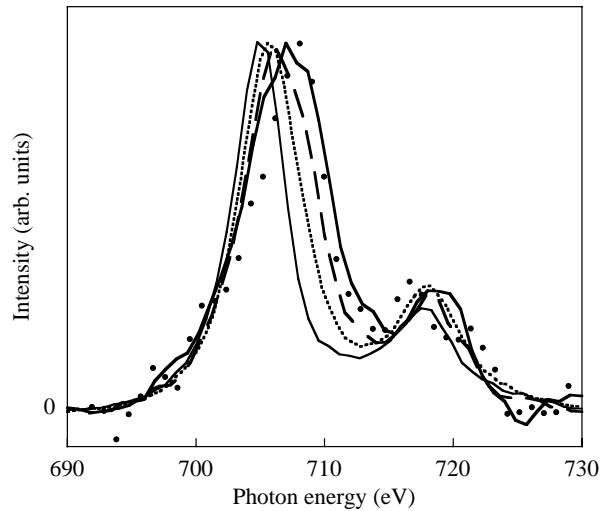


FIG. 13: Fe $L\alpha$ and $L\beta$ emissions of Fe metal, obtained with 2508 eV (thin solid line), 1208 eV (dotted line), 828 eV (dashed line), 758 eV (thick solid line), and 743 eV (dots) electrons.

of width and intensity between the two lowest electron energies may suggest an oxidation of the iron surface.

In order to determine the intensity of the satellite emission, the $L\alpha$ spectrum obtained at 2508 eV, and considered without satellite, is fitted to the low photon energy side of the spectra obtained with the lowest electron energies, as done in Ref. 16. The fitted pure spectrum is then subtracted, and the surface under the remaining satellite is measured. The corresponding values are reported in Table II. This procedure also allows to determine that the satellite lies about 3.5 eV above the normal line.

C. $5d$ transition metals (W)

The M_3O_5 emission from the W sample is shown in the Fig. 14. The spectra are obtained with 5515 and 2805 eV electrons. The intensity of this emission band is so weak that it was not possible to obtain a sufficient intensity with an overvoltage below 1.2. A polynomial of the second degree, representing the background, is subtracted. The spectra are normalized with respect to the maximum of the M_3O_5 emission, which is observed around 2275 eV. On the spectrum obtained at 5515 eV, a satellite is observed about 15 eV above the normal emission band. When the incident electron energy decreases, both parent and satellite emissions are observed but the relative intensity of the satellite increases. The intensity ratios $I(\text{parent})/I(\text{sat})$ are indicated in the Table II.

IV. DISCUSSION

For the type of experiments described above, the $4d$ transition metals are optimal. For the $3d$ elements, the

TABLE III: Photon energy shift of the maximum of the $L\alpha$ emission, $\Delta h\nu$, variation of the full width at half maximum of the $L\alpha$ line, ΔFWHM , and variation of the relative intensity of the $L\alpha$ and $L\beta$ emissions, $\Delta I(L\alpha)/I(L\beta)$, of Fe metal as a function of the incident electron energy. The parameters indicate the variation with respect to the spectrum obtained at 2508 eV. For the oxides excited by synchrotron radiation, the parameters indicate the variation with respect to Fe metal.

Electron energy (eV)	$\Delta h\nu$ (eV)	ΔFWHM	$\Delta I(L\alpha)/I(L\beta)$
2508	0	0	1
1208	+0.6	+1.1	$\times 1.0$
828	+1.0	+2.0	$\times 1.6$
758	+2.2	+3.1	$\times 2.4$
743	+3.0	+1.5	$\times 1.6$
Photon excitation			
750 eV synchrotron radiation			
Fe ^a	0	0	1
FeO ^a	+0.4	+0.8	$\times 0.5$
Fe ₂ O ₃ ^a	+1.4	+1.3	$\times 0.5$

^afrom Ref. 15.

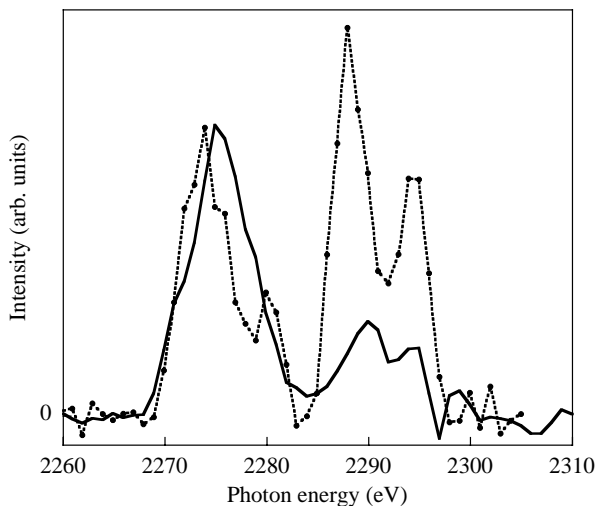


FIG. 14: $W M_3O_5$ emission of W metal, obtained with 2805 eV (dashed-dotted line), and 5515 eV (solid line) electrons.

satellite is relatively close to the parent emission band and difficult to resolve. For the $5d$ elements, both the emission band and its satellite are very weak. Therefore, most of our results concerns the $4d$ elements.

The high energy satellite of the emission bands shows the same resonant-like behaviour near the threshold, for all the transition elements studied in the present work. For the $L\alpha$ emissions, which involve an inner d subshell, the satellite does not show the intensity enhancement at the threshold. For Ag, which has no open d subshell, the satellite is not observed.

For the $4d$ transition elements, we have observed that the intensity of the satellite with respect to that of the parent line increases when the incident electron energy decreases below the $2s$ and $2p_{1/2}$ ionization limits. This clearly indicates that the initial state of the satellite is

not obtained from a Coster-Kronig process involving the $2s$ or $2p_{1/2}$ levels (Table I). The differences, $E - E_0$, between the energies of the incident electrons and the binding energies of the $np_{3/2}$ core levels are indicated in Table II for all the studied elements. These differences correspond to the energy excess available to create a supplementary excitation or ionization. As an example, for Mo, at lower incident energies, the energy excess is smaller than the binding energies of the $4s$ and $4p$ electrons (Table I). Consequently, only a valence electron can be ejected. This leads to a $d - d$ low energy excitation. Indeed, the predominant role played by the unoccupied d states in favoring the observation of the satellite, indicates the higher transition probability to these states.

All these results confirm the proposed interpretation in Ref. 2. From this, the $2p_{3/2}$ satellite of the nd transition elements is due to the decay of the doubly-excited $2p_{3/2}^{-1}nd^{-1}\epsilon d\epsilon'd$ configuration to the $nd^{-2}\epsilon d\epsilon'd$ configuration with two strongly correlated nd holes. The energies of the $L\beta_2$ satellites have been calculated by considering a supplementary vacancy in the $4d$ subshell for the elements of atomic numbers between 40 and 92.¹⁷ The calculations are made in the intermediate coupling scheme using an HFS (Hartree-Fock-Slater) program, with corrections for relaxation and solid state effects, and the obtained values are in agreement with our experimental energies (Cf. Table IV).

Information on the nd distributions can be deduced from our spectra. For the $4d$ elements and a given over-voltage, the intensity of the satellite with respect to that of the parent line is proportional to the number of unoccupied d states. On the other hand, the energy interval between the satellite and the parent line is 3-4 eV for Fe, 7-8 eV for the $4d$ elements, and 15 eV for W. This interval is almost constant along the $4d$ series. It is characteristic of the studied transition involving the nd and core subshells. Indeed, this energy interval corresponds

TABLE IV: Comparison between the experimental and theoretical energy of the maximum of the satellite line of the $L\beta_2$ band of the studied $4d$ transition metals.

Z	Element	experiment (eV)	theory (eV) ^a
39	Y	2085	-
40	Zr	2226	2229.2
42	Mo	2526	2526.5
44	Ru	2844	2842.4
47	Ag	-	3356.6

^afrom Ref. 17.

to the shift of the emission band in the presence of an additional nd hole.

To our knowledge, only two previous calculations of the satellite-parent line separation exist for the np emission bands. One of them is for the Zr $L\beta_2$ band¹⁸: the value obtained by the difference of the energies calculated for each of the emissions separately is 2.4 eV, while the experimental separation is about 7 eV. We have calculated the separation for Mo. We obtain by taking into account the correlations among all the J -levels of the various configurations involved a value of 7.2 eV,² in satisfactory agreement with the experimental value of 8 ± 0.5 eV. The other one involves the $L\beta$ emissions of the $3d$ elements.^{19,20} It was found that the satellite due to the presence of an additional $3d$ vacancy in the valence band of Fe lies about 2 eV above the parent line. This could correspond to the broadening that we have observed for the Fe $L\beta$ band (see section III B). No calculation has been made for the $L\alpha$ emission.

No theoretical model exists to describe the emission intensity in the region close to the threshold, where the correlations are strong. One expects the probability to create the doubly-excited $2p_{3/2}^{-1}nd^{-1}ede'd$ configuration of low energy to be large for the transition elements, where occupied and unoccupied d states of high density are present. Both $L\beta_2$ and $L\alpha$ satellites of the $4d$ elements have this configuration as initial state. However, we have observed that the intensity of the $L\beta_2$ and $L\alpha$ satellites varies in a very different manner close to the $2p_{3/2}$ threshold. For $L\alpha$ emissions, the parent and satellite are atomic transitions between core levels, whose intensities vary in a similar manner. The $L\beta_2$ satellite is a one-site process, owing to the presence of the two nd holes at the final state. This induces a strong enhancement of the relative intensity of the satellite with respect to that of the emission band. These results reveal the important role of the correlations between the nd holes in the valence band of the transition elements.

The intensity of the Mo $L\beta_2$ satellite relative to that of the parent line has been calculated for a 2.5 overvoltage and found equal to 6%.²¹ For a 2.4 overvoltage (6015 eV), no satellite is observed. We have tried to fit the $L\beta_2$ spectrum by taking into account the presence of a satellite at 2525 eV, *i.e.* at the position of the satellite observed at

lower electron energy. If a satellite would be present, its relative intensity would be clearly lower than 1%, a value much lower than the calculated one.

The existence of the satellite depends on the distribution of states within the valence and conduction bands: it is observed for Mo metal but not for Mo in a silicide (see Fig. 6). From calculations of the local and partial density of states for Mo and Mo_5Si_3 ,^{22,23} the number of Mo $4d$ states in the silicide is about half of that in the metal. The d states are more localized in the compound than in the metal. Thus, an excitation energy closer of the threshold should be necessary in order to observe the satellite. This could explain why the satellite is not observed with a 1.12 overvoltage.

Experiments using the synchrotron radiation have been performed with excitation energy close to the threshold of the $L\alpha$ emission of the $3d$ transition element compounds. The existence of such a satellite has already been seen,²⁴ but without any identification or discussion. It must be noted that the analyzed thickness is large in the fluorescence experiments, due to the long range of photons in the matter. Consequently, the reabsorption effect is strong for the metals at open d subshell.^{25,26} This causes strong perturbations of the emission band above the top of the valence band, where the high energy satellite is expected. So great care must be taken to avoid the reabsorption, in order to obtain reliable information about the high energy satellite by x-ray fluorescence.

The excitation under electron bombardment presents several advantages for this type of study. After an inelastic scattering by a core electron, an incident electron of initial energy near the excitation threshold is present in the excited states of low energy. No selection rule exists and all the empty states can accept the incident electron, thus simplifying the interpretation of the spectra in the region of the threshold. No shift of the x-ray emissions is expected as a function of the incident energy, contrary to what is observed in resonant x-ray fluorescence spectroscopy. Consequently, the satellite can be resolved from the parent emission. Due to the energy distribution of the incident electrons inside the sample, the excited states involved in the process are distributed on a large energy range with respect to the optical energy range. This energy distribution of the incident electrons in the sample is also responsible for the observation of the satellite in an energy range of about 100 eV above the threshold.⁷ Consequently, the x-ray emission induced by electrons is a convenient tool for studying the elementary excitations in the solid.

V. CONCLUSION

The present results show that experiments using the electron impact can be performed close to the excitation threshold of x-ray transitions. We have shown the existence of a satellite in the high energy side of the emission band of the nd transition metals. It is interpreted by

the transition $2p_{3/2}^{-1}nd^{-1} - nd^{-2}$ and is observable only when the incident electron energy is close to the ionization limit. The relative intensity of this satellite with respect to the emission band varies in an unusual manner with the incident electron energy. It is maximum for impact energy near the threshold and decreases with increasing electron energy. At higher electron energies, its intensity is very low and the satellite smears out at the foot of the parent line. We attribute this resonant-like behaviour of the intensity to the atomic-like character of the satellite with respect to the emission band and to strong correlations between d holes in the valence band. From the variation of the satellite intensity with respect to that of the emission band, information on the dynamics of the $d-d$ intraband excitations and the character of the d electrons can be deduced.

These experiments were made possible because of the fine tuning and experimental control (within a few eV) of the electron energy. The quality of the experiments is

also due to the stability of the apparatus⁸ during the data acquisition. This is mandatory to collect emission bands and satellite lines of weak intensities. This has allowed to discriminate the different behaviors of the parent line and its satellite close to the ionization limit, and to observe that the intensity of the satellite is higher than that of the normal line under these electron impact conditions.

Acknowledgments

Pr. M. Quarton, from Pierre et Marie Curie University, is acknowledged for providing us with the MoO₃ powder. Dr. A. Bosseboeuf, from the Institut d'Electronique Fondamentale, Paris-Sud University, is thanked for his preparation of the Mo and W films. The authors are grateful to Dr. N. Spector and Dr. J.-J. Gallet for fruitful discussions.

* Electronic address: jonnard@ccr.jussieu.fr

¹ C. Sternemann, A. Kaprolat, M. H. Krisch, and W. Schülke, Phys. Rev. B **61**, 020501 (2000).

² P. Jonnard, C. Bonnelle, and I. Jarrige, Phys. Rev. Lett., submitted.

³ S. M. Butorin, J. Elec. Spectrosc. Rel. Phenom. **110-111**, 213 (2000).

⁴ L.-C. Duda, T. Schmitt, A. Augustsson, and J. Nordgren, J. All. Comp. **362**, 116 (2004)

⁵ Y. Cauchois and C. Sénémaud, *Wavelengths of X-ray Emission Lines and Absorption Edges*, International Tables of Selected Constants **18**, (Pergamon Press, 1978).

⁶ J. A. Bearden and A. F. Burr, Rev. Mod. Phys. **39**, 125 (1967).

⁷ P.-F. Staub, X-Ray Spectrom. **27**, 43 (1998); P.-F. Staub, P. Jonnard, F. Vergand, J. Thirion, and C. Bonnelle, *ibid.* **27**, 58 (1998).

⁸ C. Bonnelle, F. Vergand, P. Jonnard, J.-M. André, P. Avila, P. Chargelègue, M.-F. Fontaine, D. Laporte, P. Paquier, A. Ringuenet, and B. Rodriguez, Rev. Sci. Instrum. **65**, 3466 (1994).

⁹ V. M. Cherkashenko, V. V. Shumilov, and G. V. Bazuev, Rus. J. Inorg. Chem. **39**, 1132 (1994).

¹⁰ G. Dräger, W. Czolbe, A. Simunek, and F. Lévy, Cryst. Res. Technol. **20**, 1451 (1985).

¹¹ G. F. Khudorozhko, L. G. Bulusheva, L. N. Mazalov, V. E. Fedorov, J. Morales, E. A. Kravtsova, I. P. Asanov, G. K. Parygina, and Y. V. Mironov, J. Phys. Chem. Sol. **59**, 283 (1998).

¹² C. Bonnelle, *X-Ray Spectroscopy*, The Royal Society of Chemistry, Annual Report C (1987) p. 201.

¹³ V. V. Nemoshkalenko, A. P. Shpak, and V. P. Krivitsiy, Phys. Met. Metall. **39**, 44 (1975).

¹⁴ C. F. Hague, J.-M. Mariot, and G. Dufour, Phys. Lett. **78A**, 328 (1980).

¹⁵ E. Z. Kurmaev, A. Moeves, V. R. Galakhov, D. L. Ederer, and T. Kobayashi, Nucl. Instr. Meth. Phys. Res. B **168**, 395 (2000).

¹⁶ M. Magnuson, N. Wassdahl, and J. Nordgren, Phys. Rev. B **56**, 12238 (1997).

¹⁷ S. N. Soni and M. H. Massoud, J. Phys. Chem. Sol. **58**, 145 (1997).

¹⁸ M. O. Krause, F. Wuilleumier, and C. W. Nestor Jr., Phys. Rev. A **6**, 871 (1972).

¹⁹ S. N. Soni, J. Phys. B **23**, 1117 (1990).

²⁰ S. N. Soni and S. Poonia, Ind. J. Pure Appl. Phys. **40**, 213 (2001).

²¹ S. N. Soni, private communication.

²² A. K. McMahan, J. E. Klepeis, M. van Schilfgaarde, and M. Methfessel, Phys. Rev. B **50**, 10742 (1994).

²³ I. Jarrige, PhD Thesis, Pierre et Marie Curie University, Paris, 2003.

²⁴ S. M. Butorin, J.-H. Guo, M. Magnusson, P. Kuiper, and J. Nordgren, Phys. Rev. B **54**, 4405 (1996).

²⁵ C. Bonnelle, Annal. Phys. **I**, 439 (1966).

²⁶ J. Kawai, K. Maeda, K. Nakajima, and Y. Gohshi, Phys. Rev. B **52**, 6129 (1995).